Seismotectonics of the 6 February 2012 Mw 6.7 Negros Earthquake, central Philippines

Article · December 2016

DOI: 10.1016/j.jseaes.2016.12.018

Journal of Asian Earth Sciences 142 (2017) 93–108

Contents lists available at ScienceDirect

Journal of Asian Earth Sciences

journal homepage: www.elsevier.com/locate/jseaes

Full length Article

Seismotectonics of the 6 February 2012 Mw 6.7 Negros Earthquake, central Philippines

M.A. Aurelio [a,*], J.D.B. Dianala [a], K.J.L. Taguibao [a,1], L.R. Pastoriza [b,2], K. Reyes [b], R. Sarande [c], A. Lucero Jr. [d]

[a] National Institute of Geological Sciences, Velasquez St. corner C.P. Garcia Avenue, National Science Complex, University of the Philippines, Diliman, Quezon City 1101, Philippines
[b] Energy Development Corporation, Julia Vargas Ave. Cor. Meralco Ave., Ortigas Center, Pasig City, Philippines
[c] Philex Mining Corporation (Negros Exploration Group), Brixton St., Pasig City, Philippines
[d] Mines and Geosciences Bureau, Regional Office No. 7, Mandaue City, Philippines

ARTICLE INFO

Article history:
Received 27 February 2016
Received in revised form 10 December 2016
Accepted 10 December 2016
Available online 16 December 2016

Keywords:
Mw 6.7 February 2012 Negros Earthquake
Negros Oriental Thrust
Fold-thrust systems
Basin inversion
Low strain rate
Seismic hazard assessment

ABSTRACT

At 03:49 UTC on the 6th of February 2012, Negros Island in the Visayan region of central Philippines was struck by a magnitude Mw 6.7 earthquake causing deaths of over 50 people and tremendous infrastructure damage leaving hundreds of families homeless. The epicenter was located in the vicinity of the eastern coastal towns of La Libertad and Tayasan of the Province of Negros Oriental. Earthquake-induced surface deformation was mostly in the form of landslides, liquefaction, ground settlement, subsidence and lateral spread. There were no clear indications of a fault surface rupture. The earthquake was triggered by a fault that has not been previously recognized. Earthquake data, including epicentral and hypocentral distributions of main shock and aftershocks, and focal mechanism solutions of the main shock and major aftershocks, indicate a northeast striking, northwest dipping nodal plane with a reverse fault mechanism. Offshore seismic profiles in the Tañon Strait between the islands of Negros and Cebu show a northwest dipping reverse fault consistent in location, geometry and mechanism with the nodal plane calculated from earthquake data. The earthquake generator is here proposed to be named the Negros Oriental Thrust (NOT). Geologic transects established from structural traverses across the earthquake region reveal an east-verging fold-thrust system. In the latitude of Guihulngan, this fold-thrust system is represented by the Razor Back Anticline – Negros Oriental Thrust pair, and by the Pamplona Anticline – Yupisan Thrust pair in the latitude of Dumaguete to the south. Together, these active fold-thrust systems are causing active deformation of the western section of the Visayan Sea Basin under a compressional tectonic regime. This finding contradicts previous tectonic models that interpret the Tañon Strait as a graben, bounded on both sides by normal faults supposedly operating under an extensional regime. The Negros Earthquake and the active fold-thrust systems that were discovered in the course of the structural analysis provide strong arguments for basin inversion processes now affecting the Visayan Sea Basin, albeit under very slow strain rates derived from previous GPS campaigns. The occurrence of the earthquake in an area where no active faults have been previously recognized and characterized by slow present-day strain rates underscores the necessity of paying more attention to and exerting more effort in the evaluation of earthquake hazards of regions that are seemingly seismically quiet, especially when they underlie highly urbanized areas.

1. Introduction

The island of Negros in the central Philippines was struck by a magnitude Mw 6.7 earthquake towards midday of 6 February 2012, causing extensive damage to infrastructure and killing at least 50 people living in towns settled on the eastern coast of the island. Initial calculations by several earthquake monitoring agencies including the Philippine Institute of Volcanology and Seismology (PHIVOLCS), the National Earthquake Information Center of the United States Geological Survey (NEIC-USGS) and the National Research Institute for Earth Science and Disaster Resilience (NIED) of Japan immediately after the earthquake located the epicenter a few kilometres east of the coast of central Negros, while the depth of focus was estimated at around 10 km. Although the initial focal

* Corresponding author.
E-mail address: maurelio@nigs.upd.edu.ph (M.A. Aurelio).
[1] Department of Earth Science and Technology, Akita University, 1-1 Tegata Gakuen-machi, Akita City 010-8502, Japan.
[2] Department of Earth Sciences, Sciences Labs, University of Durham, Durham DH1 3LE, United Kingdom.

http://dx.doi.org/10.1016/j.jseaes.2016.12.018
1367-9120/

mechanism solution (FMS) indicated reverse faulting, its shallow hypocentral depth and the large epicentral distance from the axis of the Negros Trench given the known subduction angle (Cardwell et al., 1980; Aurelio, 2000a), did not argue for a subduction-related earthquake that would have been generated by this trench, an east dipping subduction zone located about 100 km west of the island. Quick Response Teams (QRTs), led by government institutions that included the Philippine Institute of Volcanology and Seismology (PHIVOLCS), the Lands Geological Survey Division of the Mines and Geosciences Bureau (MGB-LGSD) and the National Institute of Geological Sciences of the University of the Philippines (UP-NIGS) deployed immediately to the ground mainly to assess damage, but also to conduct immediate co-seismic ground deformation, mostly noted the absence of a clear fault surface rupture. Prior to this earthquake, existing maps in the Philippines did not indicate the presence of any active fault that would correspond to a seismic generator. This paper presents results of a study that includes onshore structural field observations, earthquake data analysis and offshore seismic profile interpretation, in an attempt to characterize the earthquake fault, which has otherwise generated debates amongst earthquake researchers, as well as to better understand the seismotectonic setting of Negros Island in the light of the recent seismic event. This work provides valuable insights to earthquake hazard assessment, especially of regions where active faults are unknown or have not been mapped.

2. Regional tectonic setting

Earthquake-prone Philippines is surrounded by oppositely-verging subduction systems, and traversed by active transcurrent faults all throughout the length of the archipelago (Cardwell et al., 1980; Aurelio, 2000a; Aurelio et al., 2013a) (Fig. 1). To the west, 4 subduction systems dip east or southeast, namely from the north; (1) Manila Trench where the South China Sea (SCS) oceanic lithosphere is consumed underneath the Luzon Arc; (2, 3) the Negros and Sulu Trenches where the Sulu Sea (SS) oceanic lithosphere subducts underneath the Negros-Zamboanga-Sulu-Jolo Arcs; and (4) the Cotabato Trench where the Celebes Sea (CS) oceanic lithosphere underplates the Sarangani-Sangihe Arcs. To the east, the west-dipping East Luzon Trough and Philippine Trench are responsible for the sudduction of the Philippine Sea Plate (PSP) underneath the East Luzon – Bicol – East Mindanao Arc. This oppositely-dipping subduction system creates a sandwiched Philippine Mobile Belt (PMB) (Gervasio, 1967). As the PSP translates northwestwards with respect to a fixed reference point in Eurasia at an average rate between 7 cm/yr (Seno, 1977) and 10 cm/yr (Argus et al., 2011), the ensuing northwestwards dispersion of tectonic blocks within the PMB is facilitated by numerous strike-slip faults, the most prominent of which is the multi-branched sinistral Philippine Fault System (PFS) that traverses the entire length of the archipelago from Luzon in the north to Mindanao in the south for over 1200 km (Pinet, 1990; Pinet and Stephan, 1990; Ringenbach et al., 1990; Ringenbach, 1992; Aurelio, 1992; Aurelio, 2000a; Aurelio et al., 1991; Quebral, 1994). GPS-derived motion vectors and strain rates (*e.g.* Kreemer et al., 2000, 2000b; Rangin et al., 1999; Aurelio, 2000b, 2001; Yu et al., 2013) indicate that generally, blocks east of the PFS travel faster than those located west of it, with the slowest block motions observed towards the north Palawan-southwest Mindoro-northwest Panay Collision Zone (PMPCZ).

3. Tectonic setting of Negros island

Negros Island is located to the west of the PFS, and to the southeast of the PMPCZ. Its eastern third is underlain by middle to late Cenozoic sedimentary packages of the Visayan Sea Basin (Bureau of Energy Development, 1986; Porth et al., 1989), that also underlies the neighboring islands of Cebu and Bohol. The rest of the island is composed of an active volcanic arc superimposed over older volcanic arcs mostly dominated by metalliferous late Oligocene to Pliocene intrusions and their equivalent extrusives (Aurelio and Peña, 2010) (Fig. 2). This active volcanic arc, represented by 3 andesitic strato volcanoes from north to south by Mt. Mandalgan, Mt. Kanlaon and Mt. Cuernos de Negros, is associated to the east-dipping Negros Trench which is the closest known active subduction zone located about 100 km to the west. Prior to the earthquake, there were no known active faults traversing the island, based on official active fault maps (PHIVOLCS, 2000). Otherwise, faults have been inferred to exist in certain locations on the island but these have yet to be confirmed by further studies. However, field observations during this work and geologic maps of the island (Aurelio and Peña, 2010) indicate the presence of Pliocene – Quatenary sedimentary formations and carbonate terraces presently located at relatively elevated positions (see Section 7), suggesting uplift in the recent geologic past. This observation conforms to those seen to affect sedimentary packages in the offshore region (Tañon Strait) of the Visayan Sea Basin (Rangin et al., 1989). Motion vectors derived from GPS measurements (Aurelio, 2000b; Rangin et al., 1999; Kreemer et al., 2000), when fixed relative to Palawan Island in western Philippines, indicate that Negros island, like the neighboring islands of Panay, Cebu and Bohol is moving at a slower northwestward rate than blocks located further to the east. This low translation rate is generally interpreted as the result of the effect of impingement of the North Palawan Block (NPB), a buoyant microcontinental lithosphere that rifted from mainland Asia (Holloway, 1982; Hall, 2002), against the western edge of the PMB in central Philippines. Consequently, GPS-derived strain rates are likewise relatively low in the vicinity of continental impingement (Rangin et al., 1999; Kreemer et al., 2000).

4. Earthquake data

4.1. Epicentral location and depth of focus

While there was a discrepancy in the locations calculated by different seismological observatories worldwide (used in this work were those by the Global Centroid Moment Tensor Project - GCMT and PHIVOLCS) immediately after the earthquake, these seismic observatories indicated that the epicenter of the main shock was located near the coast between the towns of La Libertad and Tayasan. The depth of focus was estimated to be between 10 and 15 km. Given the localized and denser seismic network of PHIVOLCS, the epicentral locations of the main shock and aftershocks calculated by this observatory is preferred over the others that based their solutions from the more dispersed and less dense global seismic network.

4.2. Focal mechanism solution and aftershock distribution (fault strike, dip, rake)

Considered in this study are FMS calculations by the NIED and GCMT (Dziewonski et al., 1981; Ekström et al., 2012). Earthquake parameters of the main shock by GCMT provide nodal planes with strike/dip/rake measurements of 210°/47°/97° and 19°/43°/83°, while NIED provides 180°/45°/60° and 35°/52°/117° respectively. The northeasterly distribution of seven-day aftershock epicenters appears more consistent with the GCMT solution that identifies a NE-SW (210°) striking fault (Fig. 3), which corresponds to the southeast-dipping nodal plane of the NIED FMS, as opposed to the west-dipping, N-S (180°) striking fault. Likewise, hypocentral

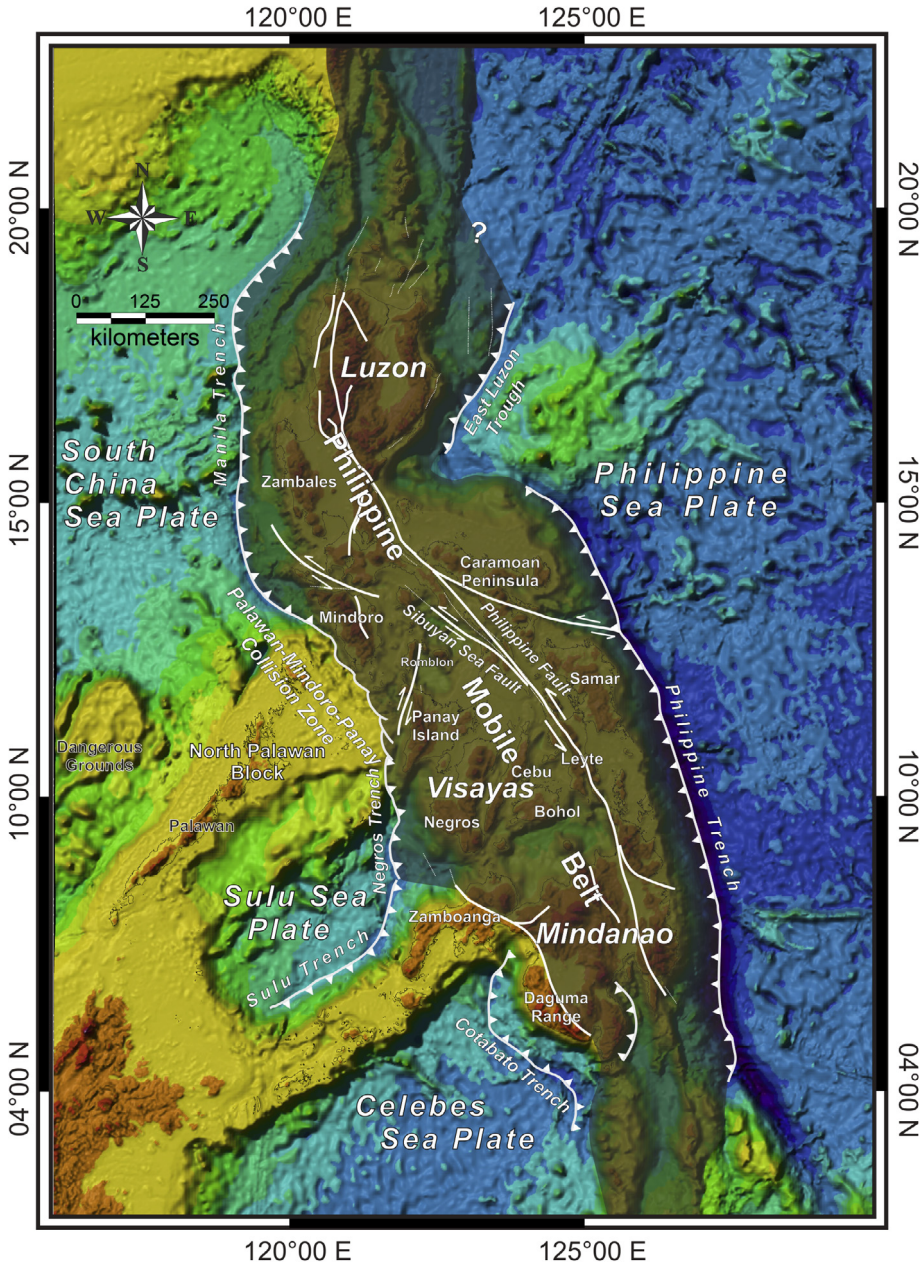

Fig. 1. Simplified tectonic map of the Philippines showing the salient features including the 6 subduction zones and major actives faults surrounding and criss-crossing the archipelago respectively. Also shown are the 2 major terranes of the Philippine Mobile Belt (PMB) and the micro-continental North Palawan Block (NPB). Negros Island is located to the southeast of the PMB – NPB Collision Zone (PMPCZ).

plot of the aftershocks, considering errors in location both horizontally and vertically, indicate preference to a northwest-dipping plane consistent with the GCMT solution. These readings suggest that the preferred rupture plane strikes NE-SW (210°) and dips 47° to the northwest. The high angle rake of 97° implies an almost reverse fault mechanism, with a small right-lateral displacement. However, in an area with no previously mapped active faults, these limited seismological observations are not fool proof in determining the attitude of the rupturing fault. Nevertheless, aftershock distribution is indicative of the main fault area (Das and Henry, 2003), and can guide the investigation of deformation in the field.

5. Earthquake-induced ground deformation

Field investigation starting 2 days after the earthquake did not yield a clear manifestation of a fault surface rupture associated to a NE-SW striking reverse fault, as suggested by the computed FMS and the configuration of the aftershock distribution. Instead, earthquake-induced ground deformation was mostly manifested in the form of landslides, liquefaction, differential settlement and similar ground behaviour in response to intense ground shaking. Such observations are consistent with those gathered by the QRTs of PHIVOLCS (Abigania et al., 2012; Bacolcol et al., 2012; Daag et al., 2012), MGB (Gemal et al., 2012) and UP-NIGS (Aurelio et al., 2012).

5.1. Landslides

The Negros earthquake induced numerous landslides over an area more than 40 km long and about 10 km wide, from the town of Valle Hermoso in the north to the town of Ayungon in the south (Fig. 4). The surface area of landslides that caused significant damage ranges in size from a few square kilometres to a few tens of

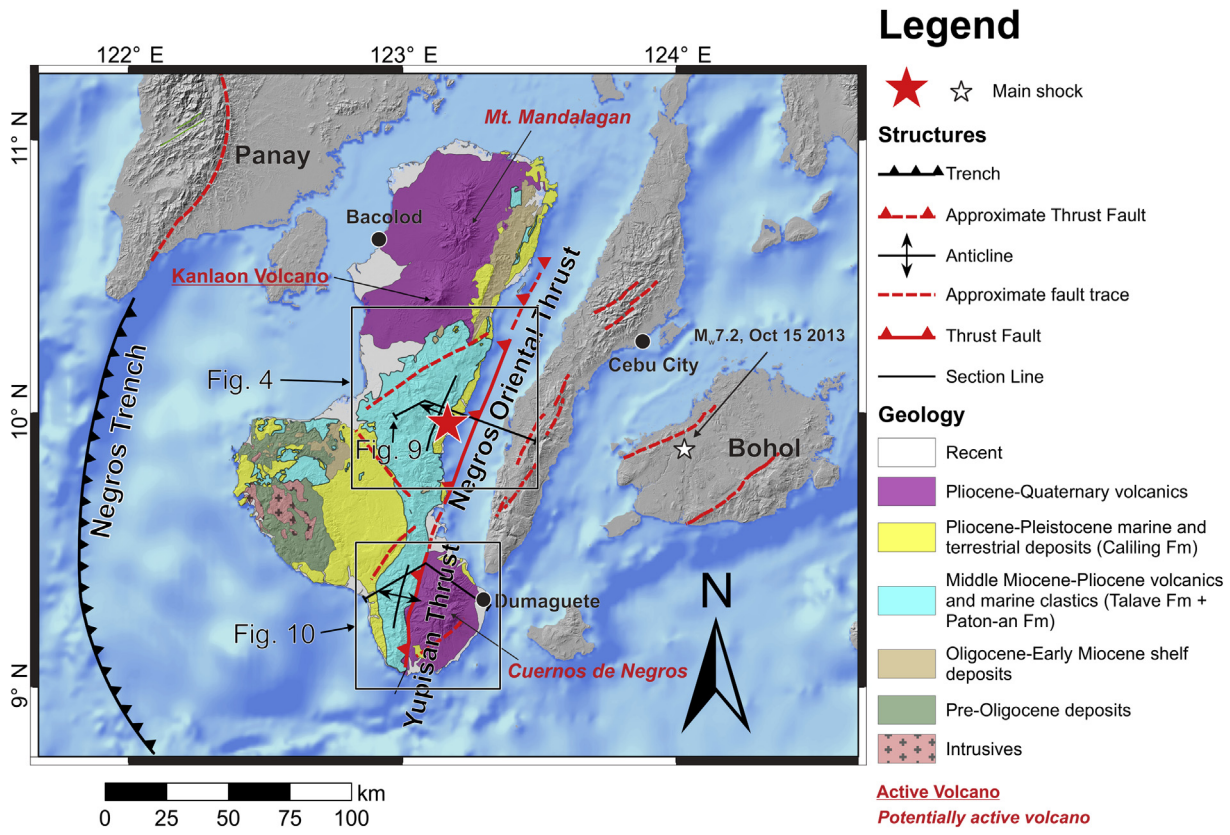

Fig. 2. Localized tectonic map of Negros and surroundings, showing simplified geology of the island (modified from Aurelio and Peña, 2010). Active fault and volcano data from PHIVOLCS (2012). Also shown are geologic structures established in this study with proposed names. Areas covered in Figs. 4 and 10 are indicated.

square metres (Fig. 5). The largest documented landslide was located in the upland village of Planas in the town of Guihulngan (Fig. 5a) where the landslide crown extended over 1.0 km in length. This landslide was initiated on a plane defining the contact between 2 lithological formations namely: the Caliling Formation and the Paton-an Formation, composed of rock types with differing physical properties (see Section 7). Vertical displacements on slide surfaces were observed to be as large as several tens of metres best manifested in the form of a rural road in the village of McKinley in the town of Guihulngan, dislocated vertically for about 20 m (Fig. 5b). Lateral movements were observed to extend several hundred metres as observed in the same vicinity (Fig. 5c). Numerous landslides occurred along calcareous sedimentary layers whose bedding dip directions parallel the slope (*i.e.* daylighting), rendering the bedding planes as favourable slip planes. This was best exemplified in the Solonggon Landslide (Fig. 5d) in the town of La Libertad which was initiated along southeast-dipping planes of interlayered calcareous sandstone and siltstone beds of the Caliling Formation (see Section 7). In the Razor Back Mountains (Fig. 5e), the numerous rill landslides that affected the steep eastern flank of the inherently cliff-forming reefal limestone mountain range indicate the strength of ground shaking. In the offshore area, submarine landslides have been observed using high resolution reflection seismic profiling (Daag et al., 2012). These offshore landslides are believed to have generated minor tsunami events observed by locals in the towns of Guihulngan, La Libertad and Jimalalud.

5.2. Liquefaction

Liquefaction was widespread in coastal towns due to their location at the delta of major river systems. Fig. 6a, showing an aerial view of the mouth of the river in the town of La Libertad, indicates the extent of liquefied ground indicated by the saturated sandy area on the right third of the photograph measuring several square kilometres. Damage on residential dwellings, mostly built of reinforced concrete, manifested in the form of tilted and twisted columns and shattered shear walls (Fig. 6b) suggesting a highly attenuated ground during the earthquake. Liquefaction-induced damage on horizontal infrastructure, such as bridges, manifested in the form of tilted columns and dismembered spans. Fig. 6c shows the Pangaloan Bridge in Jimalalud town affected by domino-type collapse due to tilting of the central column which was founded in saturated, predominantly sand-based foundation material weakened by shaking during the earthquake. Downtown Guihulngan is built over predominantly sandy to silty river and coastal deposits. The coastal road built on saturated, sandy and silty backfill material reacted to liquefaction by localized bulging at certain sections (Fig. 6d) that may be mistaken as reverse faulting scarps, and in other sections by uplifts and depressions (Fig. 6e) and lateral displacements of the asphalt pavement (Fig. 6f) which may be misinterpreted as strike-slip surface rupture.

5.3. Differential settlement and lateral spread

The Pangaloan Bridge in the town of Jimalalud (Fig. 6c), aside from having suffered from liquefaction, also showed indications of having been subjected to differential settlement. This soil behaviour is best observed in the domino-effect mechanism of the collapse of the bridge, as well as in the significant vertical displacement between the approach and main bridge span observed in another bridge (Bonbon) located north of Guihulngan town (Fig. 7a). Lateral spread in roads was very common for at least half the length of the area affected by earthquake-induced

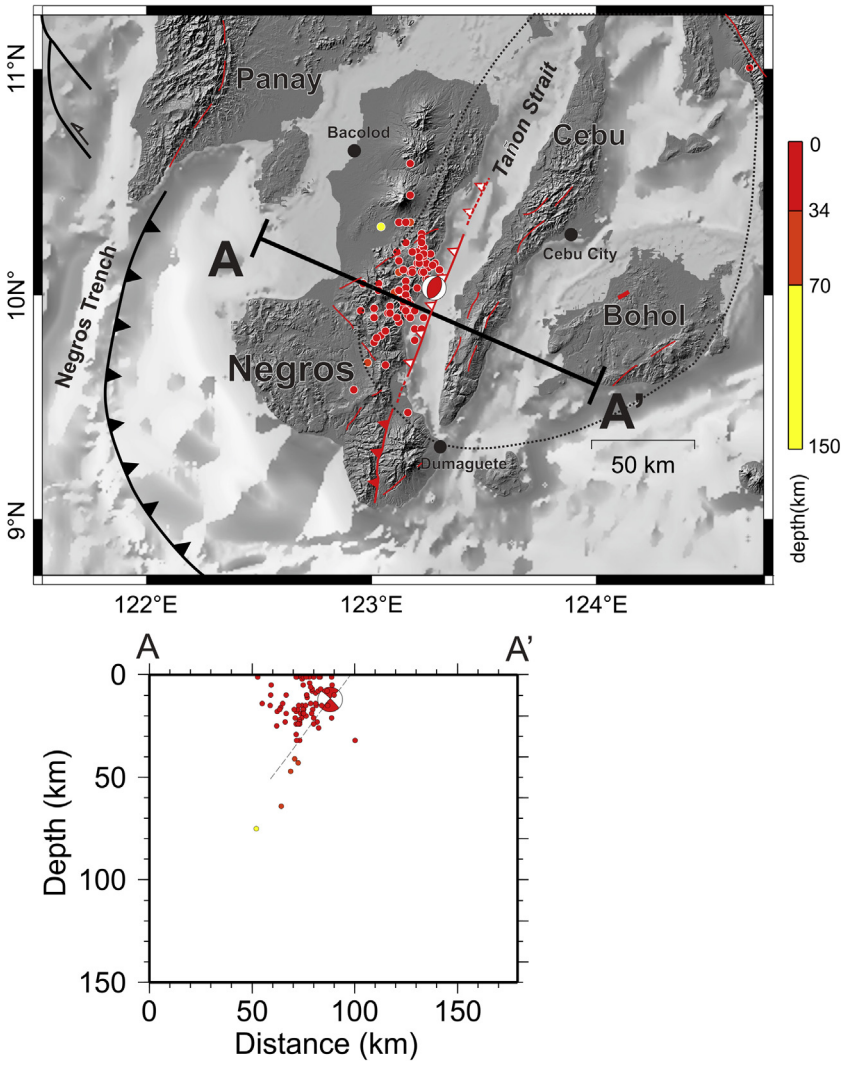

Fig. 3. Earthquake data map and section showing plot of epicenters of the main shock of 6 February 2012 and 7 days of aftershocks, and focal mechanism solution of the main shock. Earthquake data sources: Philippine Institute of Volcanology and Seismology (PHIVOLCS), Global Centroid Moment Tensor (GCMT) Project. Note the northeasterly trend of the aftershock epicentral distribution suggesting the strike of the rupturing fault, and a northwest dip suggested by the hypocentral distribution. This geometry is consistent with the attitude of the nodal plane indicated by the focal mechanism solution (FMS). Structural legend same as in Fig. 2. The extent of the Visayan Sea Basin (based from Aurelio and Peña, 2010) is shown by dotted lines on the map, encompassing eastern Negros, the entire island of Cebu and majority of Bohol.

ground deformation (from Guihulngan to Ayungon), the most notable of which were found in the towns of Guihulngan, La Libertad and Jimalalud (Fig. 7b–d).

While certain authors claim the presence of a co-seismic fault surface rupture on the basis of field observations conducted almost a year after the earthquake (*e.g.* Rimando et al., 2013), the ground deformation manifestations observed immediately after the seismic event (*e.g.* Abigania et al., 2012; Aurelio et al., 2012; Bacolcol et al., 2012; Daag et al., 2012; Gemal et al., 2012) strongly suggest that the earthquake did not produce any clear fault rupture at the surface inland. This does not however discount the possibility of a surface rupture in the offshore area.

6. Seismic profiles

The absence of a clearly defined co-seismic fault surface rupture presents difficulties in characterizing the earthquake parameters of the generator, including its strike, dip and slip mechanism. Deep-penetration seismic profiles shot in the Tañon Strait between the islands of Negros and Cebu and made available by the Department of Energy (DOE) of the Philippines provide an opportunity to image the subsurface underneath the earthquake region down to several kilometres depth. This is particularly important since the hypocentral depth is estimated between 10 and 15 km.

Since the 2-D seismic profiles were provided in their SEG-Y time-formats, it was necessary to convert them to depth sections for purposes of this study. Since most of the area in the Tañon Strait has undergone complex structural deformation, simple wave functions could not be used to adequately estimate seismic velocities that vary greatly with depth and position with respect to deformation zones. In this paper, the time-to-depth conversion procedure required the process of model-building using the "layer cake" conversion method as discussed by Marsden (1989). In this method, each seismic unit is treated separately and assigned an appropriate interval velocity. Since the 2-D seismic profiles were spaced significantly away from each other (more than 1 km), it was necessary to generate velocity models for each of them. Appropriate interval velocities were assigned using seismic velocity data derived from well data of equivalent lithologies in nearby areas within the Visayan Sea Basin (BED, 1986) and employing the method discussed by Bourbie et al. (1987). The resulting profiles are depth-converted sections. Their interpretations are discussed below.

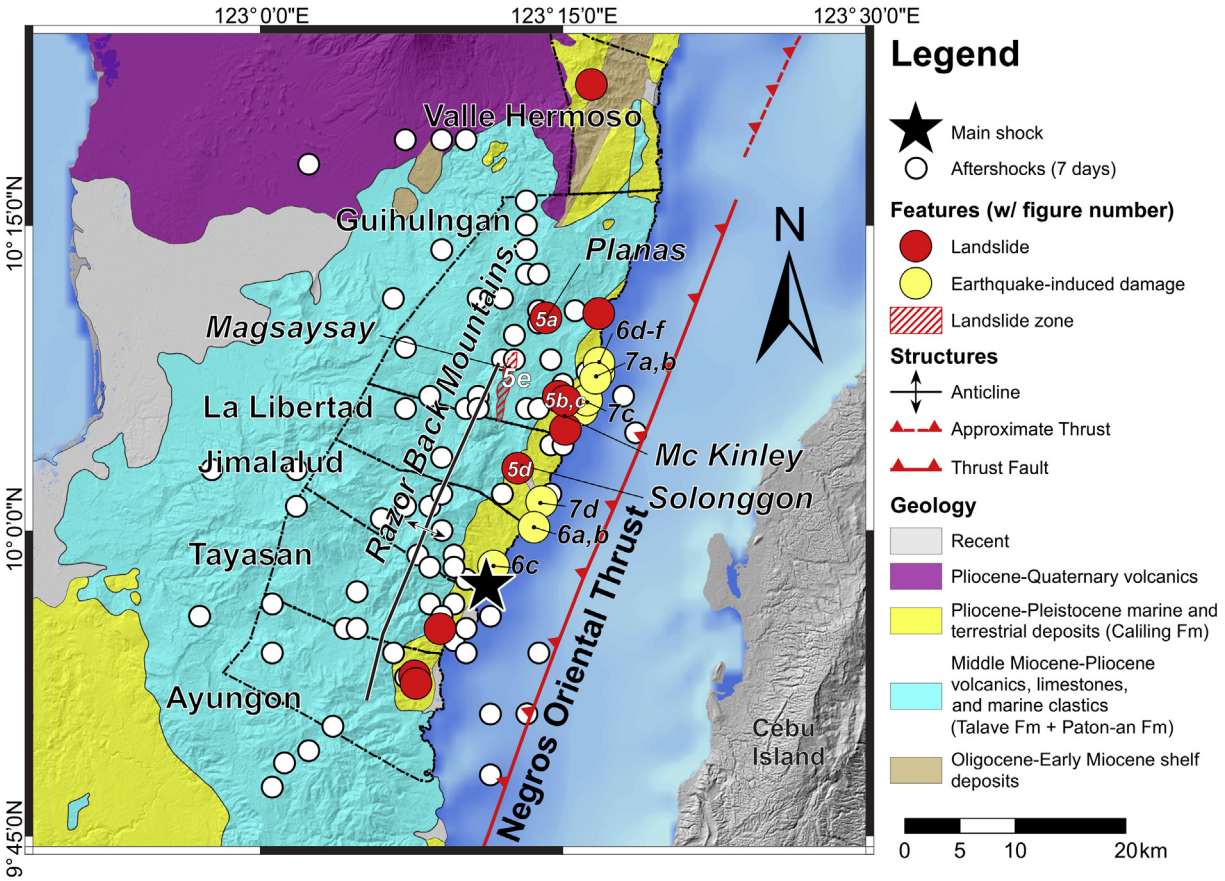

Fig. 4. Zoomed-in area of a portion of Fig. 2 showing the location of the main shock of the magnitude 6 February 2012 Negros Earthquake and distribution of 7 days of aftershocks. Also shown are the locations of observed earthquake-induced ground deformation, including landslides and other shallow-surface deformation such as liquefaction, ground settlement and lateral spread. Numberings on the circles correspond to numbered photos of ground deformation processes detailed in Figs. 5–7. Place names discussed in text are also indicated.

The Tañon Strait is underlain primarily by Cenozoic sedimentary packages that occupy the western section of the Visayan Sea Basin (Porth et al., 1989; Rangin et al., 1989; BED, 1986). While early authors (*e.g.* Glocke, 1980; Rangin et al., 1989) interpreted the strait as a northerly elongated graben bounded by normal faults on both flanks to the west and east implying an extensional tectonic regime, more recent seismic profiles suggest the presence of compressional structures in the form of anticlines and reverse faults. Fig. 8 shows several seismic lines shot in the vicinity of the epicentral area, oriented obliquely with respect to the projected strike of the rupturing fault. In the southernmost seismic line (Fig. 8A), the northwest half of the section shows a northwest-dipping reverse fault (F1) that cuts through a series of seismic reflectors down to 8.0 km and beyond, but does not penetrate the uppermost sedimentary units as it terminates at around 1.2 km from seabed. An oppositely-dipping reverse fault (F2) further to the northwest cuts through the sedimentary package from about 1.0 to 6.0 km depth. The vertical distance observed to separate reflectors that define the top and bottom of the Middle Miocene package as identified by BED (1986) suggests an estimated average vertical displacement of 1.0 km along the fault (*i.e.* 800 m at its top, 1.2 km at its bottom). A broad anticline develops between the reverse fault pair, giving rise to uplifted stratified layers at the fold crest. Although thrust fault F1 does not appear to deform the layers above its upper tip, the folded strata in the hanging wall suggest that folding is relatively recent, if not, active. Onshore, these folded layers correspond to uplifted calcareous sediments exposed along coastal towns in eastern Negros (see Section 7).

An average vertical displacement along fault F1 of about 1 km affects the Pliocene – Miocene boundary (Fig. 8A). Assuming that reverse displacement along this fault, which dips around 60° NNW, started immediately after Miocene (~5 Ma) and continued until present times (*i.e.* active fault), the average fault slip rate would be very low at about 0.23 mm/yr. Also, average strain rates calculated from GPS measurements in the Philippines are in the order of $4.0 \times 10^{e-7}$/yr. In particular, strain rates in the Negros-Cebu-Bohol region are as low as $1.0 \times 10^{e-7}$/yr (Kreemer et al., 2003). These values argue for a very slowly deforming (*i.e.* compressive) zone.

Eastwards into the strait the seismic reflectors exhibit relatively flat to very gentle inclinations. Further east however, reflectors recognized on a seismic line located northeast of that shown on Fig. 8A, start to attain northwesterly dips, peaking just west of the island of Cebu where another anticline is developed (Fig. 8B). A southeast-dipping fault (F4) appears to serve as a sole thrust affecting the basement of this broad anticline. On the northwest half of this seismic line, the northwest-dipping reverse fault seen on the line shown on Fig. 8A becomes less significant, as manifested in a northwest-dipping reverse fault (F1) which can be traced upwards beyond the Miocene – Pliocene interface. Further upwards of this interface, the Plio-Pleistocene sedimentary packages are folded to form anticlines from about 1.0 km to 3.0 km depth, with the southeastern limb accommodating compressional deformation induced by the reverse fault in the form of flexure folds, suggesting continued straining upwards into the younger sedimentary sequence. This strongly suggests that these folds are active and growing (active growth folds). At least one more northwest-dipping fault appears to flank the main reverse fault to its southeast (F3). On the basis of its orientation and the nature of displacement on the affected seismic layers, this fault appears to displace in a reverse mode, suggesting that it is oper-

Fig. 5. Earthquake-induced landslides documented in this study. (a) Landslide in the uphill village of Planas of Guihulngan town, the largest observed in this study, with a crown arc-length of more than 1 km. Photo taken from a vantage point more than 5 km away. (b) Road displaced vertically by more than 20 m by landslide in the uphill village of McKinley, Guihulngan town. (c) Top view of the same slide in (b), showing the extent of its lateral movement of the sliding mass. (d) Landslide in the village of Solonggon in La Libertad town, facilitated by daylighting bedding planes, burying more than 20 families. (e) Cliff-forming reef limestone of the Razor Back Mountain Range affected by numerous rill landslides (white, near-vertical streaks on the steep face of the mountain). See Fig. 4 for location of photos and localities mentioned.

ating under the same compressional regime that generates the main reverse fault.

The strength of reverse faulting on F1 however diminishes to the north, as can be observed on a seismic profile shown on Fig. 8C. Here, the reverse fault can be seen to vertically displace the top of the Middle Miocene reflector (BED, 1986) by about 700 m. Deformation above the fault is manifested in the form of gently tilted beds forming very broad anticlines, with significantly gentler limb inclinations than those observed in seismic lines **A** and **B**. This further argues for a decreasing reverse faulting strength northwards.

7. Structural transects

During separate campaigns, structural fieldworks were carried out to establish structural transects along lines oriented roughly perpendicular to fault strike. One transect, in the latitude of Guihulngan (Fig. 2), was established at the time earthquake damage was being assessed a few days after the tremor. Another field campaign, between the towns of Sta. Catalina and the city of Dumaguete, via Pamplona in southern Negros, was undertaken mainly to understand the structural setting of the area located south of the southernmost observed aftershock epicenter. Both transects traverse sedimentary sequences which are the equivalents of the seismic sequences delineated in the seismic profiles (see Section 6).

7.1. Razor Back Mountain – Coastal Guihulngan Transect: Razor Back Anticline – Negros Oriental Thrust system

An east-west transect from the Razor Back Mountains to the coastal town of Guihulngan reveals broadly folded Middle Miocene to Pleistocene limestones and calcareous clastic sequences (Fig. 9).

Fig. 6. Areas affected by liquefaction as a result of intense ground shaking. (a) Aerial view of the coast of La Libertad town located on a delta showing liquefied ground. (b) Damaged house resulting from column failure due to liquefaction in La Libertad town. (c) Structural failure (tilted columns, dismembered spans) on the Pangaloan Bridge in Jimalalud town induced by a combination of liquefaction and differential settlement. Damage on the coastal road of Guihulngan near the town center, including buckling (d), uplifts and depressions (e), and horizontal displacements (f) which may be mistaken as strike-slip ground rupture because they are incoherent. See Fig. 4 for location of photos and localities mentioned.

High up in the upland village of Magsaysay of Guihulngan town, a calcareous sequence composed mainly of bedded limestone, calcarenite and marl form conical karstic mounds at high elevations (>800 masl) (Fig. 9a). At this altitude, these units, belonging to the Middle to Late Miocene Talave Formation of Corby et al. (1951 *in* Aurelio and Peña, 2010), exhibit beds that are particularly flat-lying. Further to the east, these same bedded limestone sequences start exhibiting very gentle dips toward the east and southeast (Fig. 9b). At lower elevations but still on the slopes of the Razor Back mountain range located to the east of the bedded limestone of the Talave Formation, beds of the overlying clastic deposits, made up mostly of calcareous sandstones and siltstones and minor conglomerates, attain relatively larger but still gentle dip angles (~15°) (Fig. 9c). These predominantly fine-grained clastic sequences belong to the Early Pliocene Paton-an Formation of Melendres and Barnes (1957 *in* Aurelio and Peña, 2010). In the coastal area, outcrops expose the youngest deposits composed mainly of massive to bedded coralline limestone belonging to the Late Pliocene to Pleistocene Caliling Formation (Castillo and Escalada, 1979 *in* Aurelio and Peña, 2010). Dip angles significantly increase to more than 30° to the east (Fig. 9d). These observations suggest an anticlinal structure where the oldest rock units are exposed at the crest, while the youngest sequences flank its eastern (and western) limbs. Using the general strike of beds, the anticlinal axis is oriented north-northeasterly (around N30°), parallel to the strike of the reverse fault nodal plane (see Section 4.2 and Figs. 2 and 4). We propose to name this fold-thrust pair the Razor Back Anticline – Negros Oriental Thrust (RBA-NOT) system.

Fig. 7. Differential settlement and lateral spread. (a) Extent of vertical displacement due to differential settlement, manifested at the joint section between the approach and span of the Bonbon Bridge located north of Guihulngan town. (a_1) is a magnified view of inset box in (a). View looking east. (b) Damage on highway between the towns of Guihulngan and La Libertad resulting from a combination of ground settlement and lateral spread, view looking west. Textbook examples of lateral spread observed in the towns of Guihulngan (c – view looking NW), and Jimalalud (d – view looking NE). See Fig. 4 for location of photos and localities mentioned.

7.2. Sta, Catalina – Pamplona – Dumaguete Transect: Pamplona Anticline – Yupisan Thrust system

The western section of southern Negros is underlain by the same calcareous clastic sequences underlying the Razor Back Mountain – Guihulngan area. The eastern section is underlain by a young volcanic edifice intruding these clastic sequences, giving rise to the ellipsoidal geometry of the southern section of the island. A transect established from the town of Sta. Catalina on the west to the city of Dumaguete on the east, passing through the town of Pamplona shows the type of deformation affecting the underlying rock units.

On the western coast of Sta. Catalina, gentle westerly and northwesterly dips characterize young coralline limestones belonging to the Late Pliocene to Pleistocene Caliling Formation (Fig. 10a). Uphill to the northeast, poorly- to moderately-compacted sandstone–siltstone interbeds of the Early Pliocene Paton-an Formation underlie conformably the Caliling Formation and exhibit similar westerly and northwesterly dips (Fig. 10b). On the southwest flank of the Pamplona Ridge, semi-indurated calcareous sandstone-siltstone-mudstone interbeds belonging to the Middle to Late Miocene Talave Formation, the oldest outcropping formations along this transect, are observed to acquire gentle dips to the east and southeast (Fig. 10c). At the peak of the ridge west of the town proper of Pamplona, this same Talave Formation is characterized by numerous thrust faults and associated folds (Fig. 10d), suggesting significant compressional stresses. At the immediate vicinity east of the ridge peak, the Early Pliocene Paton-Formation reappears in the form of steep east-dipping to almost vertical beds (Fig. 10e). Further to the east into the valley between the Pamplona Ridge and the volcano, pyroclastic sands belonging to the Pleistocene to Quaternary Cuernos de Negros Volcanic Complex are observed to acquire similar steep easterly dips (Fig. 10f).

This structural configuration defines an asymmetrical anticline, here proposed to be named the Pamplona Anticline, cored by the Middle to Late Miocene Talave Formation (Fig. 10). The western limb, exposing the conformable sequences of the Early Pliocene Paton-an Formation and the Late Pliocene to Pleistocene Caliling Formation, dips gently to the west and northwest while the eastern limb is defined by easterly to southeasterly, steeply dipping beds of the Early Pliocene Paton-an Formation. This distinction between gentle and steep dip angles on the western and eastern limbs respectively suggests a west-dipping axial plane giving rise to the fold asymmetry. The presence of steeply east to northeast dipping, but much younger volcanic ash and sand deposits of the Pleistocene to Quaternary Cuernos de Negros Volcanic Complex directly in contact with steeply dipping Middle to Late Miocene Talave Formation suggest the presence of an important structure bounding these two formations. This structure, here proposed to be named the Yupisan Thrust after the village where the steeply dipping beds are best exposed (Fig. 10e), appears to play an important role in the folding process by serving as the sole thrust of the

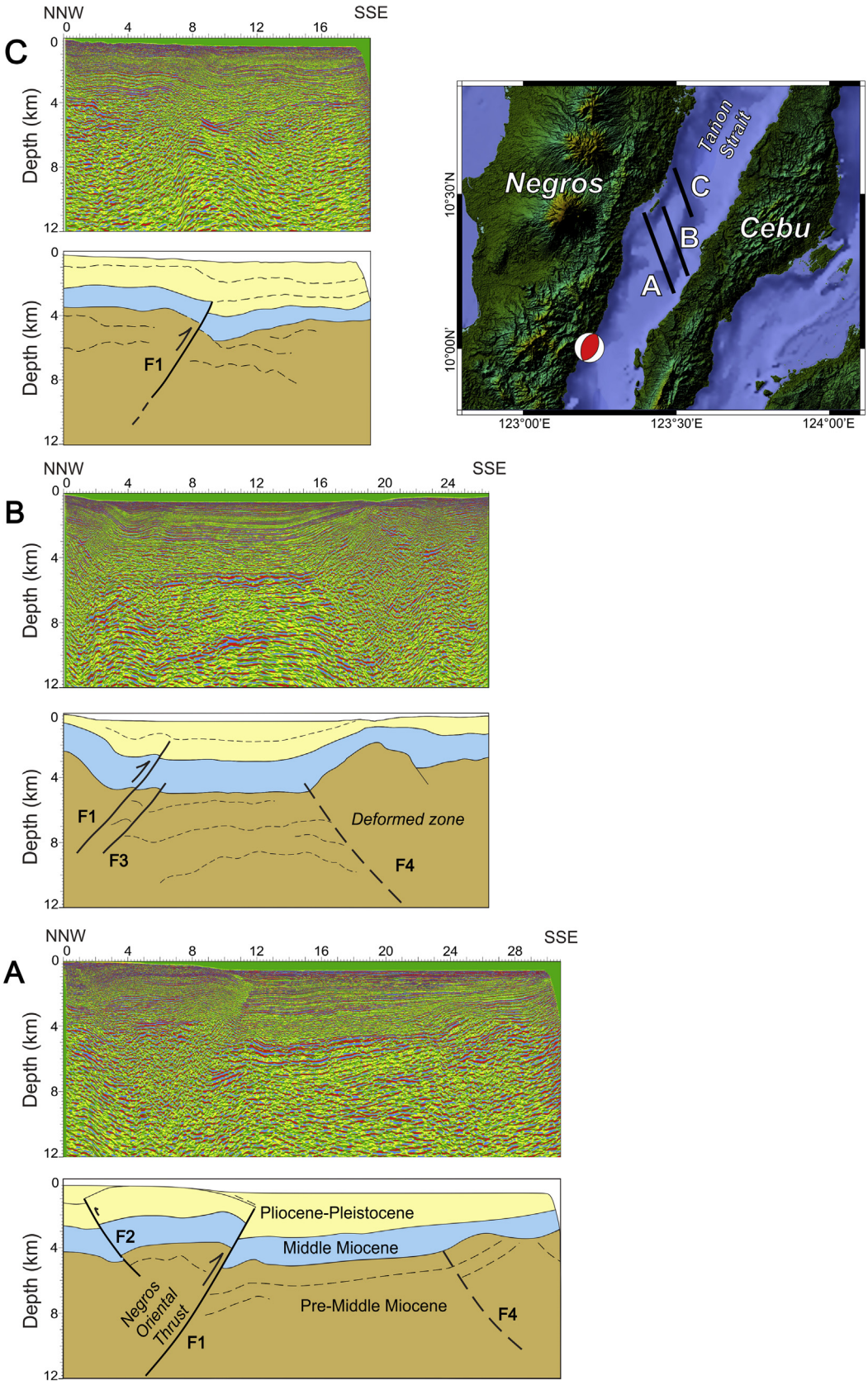

Fig. 8. Selected depth-converted offshore seismic reflection data (processed lines + interpretation, no vertical exaggeration) in the Tañon Strait, from around the latitude of Guihulngan northeastwards, showing: (A) a northwest-dipping reverse fault (F1) penetrating through the Late Miocene – Pliocene boundary but not through the most recent deposits. An oppositely verging reverse fault (F2) is observed to behave similarly further to the northwest; (B) the same northwest dipping reverse fault (F1) seen to be flanked by at least one other northwest-dipping reverse fault (F2). Further to the east towards Cebu Island, an anticlinal structure is floored by a southeast-dipping fault (F4) that also shows indications of reverse motion; (C) the same reverse fault (F1) now observed to be less significant. Fault F1 appears to correspond to the offshore signature of the Negros Oriental Thrust (see Section 7).

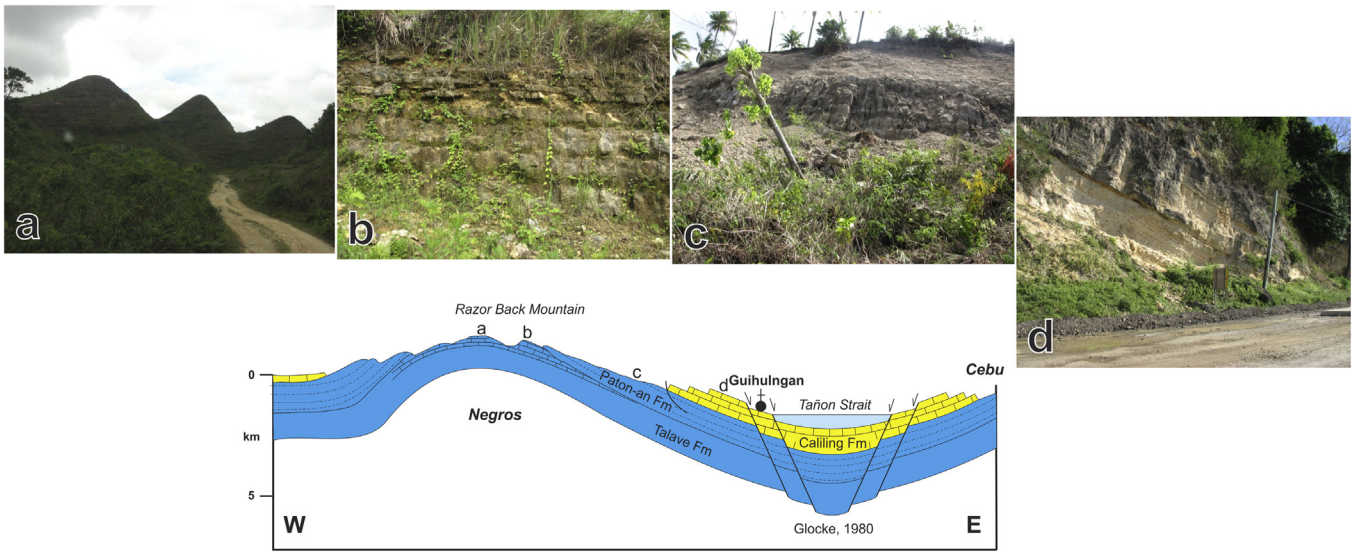

Fig. 9. Anticlinal structure established from a structural transect from the Razor Back Mountain (west) to the coastal town center of Guihulngan (east) (see Fig. 2 for approximate location of section line), manifested in the form of: (a) karstic (conical hills), flat-lying, bedded limestone and calcareous clastic deposits of the Middle to Late Miocene Talave Formation, exposed in the high altitude village (>800 masl) of Magsaysay, Guihulngan town (along the Razor Back Mountain Range axis); (b) flat-lying to very gently (east) dipping bedded limestone of the Middle to Late Miocene Talave Formation, exposed on the upper eastern flanks of the Razor Back Mountain Range; (c) gentle to very gentle easterly to southeasterly dips (30–15°) affecting bedded clastic sequences of the Early Pliocene Paton-an Formation; (d) moderately dipping (~45°) calcareous clastics and bedded and coralline limestones of the Late Pliocene to Pleistocene Caliling Formation. Graben interpretation of Tañon Strait is from Glocke (1980), but see discussions in Sections 6 and 7.1.

advancing fold as in an east-verging fold-thrust system (Fig. 10). Further to the east on the western flank of the Pleistocene to Quaternary Cuernos de Negros volcanic edifice, thick, poorly consolidated pyroclastic deposits composed mainly of laharic and tuffaceous deposits, regain gentle dips and drape over the volcanic flank.

Given its attitude with a projected northeasterly strike and a northwesterly dip and its alignment with the elongation axis defined by the aftershocks of the 2012 Negros Earthquake, the Yupisan Thrust is a favourable candidate for the southern extension of the structure that generated the Negros Earthquake (Fig. 2). The massive Cuernos de Negros Volcanic Complex appears to serve as an eastern abutment, anchoring folding and thrusting to the east. The Pamplona Anticline – Yupisan Thrust (PA-YT) system is the southern equivalent of the RBA-NOT system (Fig. 2).

8. Coulomb stress change analysis

Initial results of Coulomb static stress transfer analysis for the Negros Earthquake indicate an increase of stress in southern Negros Island in the vicinity of the Yupisan Thrust, as well as in the northern segment of the Negros Oriental Thrust (Fig. 11). Stress changes affect the probability of earthquake occurrence (Steacy et al., 2005), and stress transfer modelling in fault systems with well-studied active tectonics, like the North Anatolian Fault (Stein et al., 1997), has shown some success in identifying faults that have been promoted to failure. Faults with increased stress are brought closer to failure and can cause increased seismicity, while decrease in stress can promote the opposite (Freed, 2005; Stein, 1999; Toda et al., 2012). Coulomb stress change is quantified as $\Delta\sigma_f = \Delta\tau + \mu'\Delta\sigma_n$, where $\Delta\tau$ is change in shear stress, $\Delta\sigma_n$ is change in normal stress, and μ' is effective friction coefficient (Harris, 1998).

Calculation of co-seismic stress changes caused by the 2012 Negros Earthquake with the source fault geometry scaled to moment magnitude (Wells and Coppersmith, 1994) and using the *Coulomb* 3.3 software (Toda et al., 2005) indicate a 30-km long fault plane for a Mw 6.7 fault (Fig. 11). This is significantly shorter than a rupture length based on a seven-day aftershock distribution and the observed earthquake-related surface deformation, *i.e.*, landslides, liquefaction, and differential settlement, of more than 40 km (see Section 5). However, these are likely also indefinite basis for rupture length due to the fact that seismicity may not exactly be from the main rupturing plane. Likewise, features and processes such as landslides and liquefaction may be controlled by other factors like bedrock type and peak ground acceleration. With the lack of clear indications of fault geometry from an actual surface fault rupture, the conservative geometry of the empirically-derived fault is satisfactory for a simple stress transfer model. The attitude of this fault (strike = 210°, dip = 47°, and rake = 97°) is based on the NW-dipping nodal plane of the FMS derived by Global CMT, with the center relocated to the epicenter calculated by PHIVOLCS to fit the attitude of the Negros Oriental Thrust. The following *Coulomb* parameters were then used for the modelling, namely; uniform elastic half-space based on Okada (1992), Young's modulus of 8×10^4 MPa, and Poisson's ratio to 0.25 (*e.g.* Stein et al., 1992; Toda and Stein, 2013). With the range of effective friction coefficient usually ranging from 0 to 0.8, it was set to 0.4 since exact values in the study area are unknown. This value also was used to minimize uncertainty (Toda and Enescu, 2011; Toda et al., 2011). Stress was calculated on specified receiver reverse faults, in a 10 × 10-km grid, that have similar attitudes to the Negros Oriental Thrust and the Yupisan Thrust, both of which strike NNE and have moderate dips to the northwest.

Analyzing the distribution of seismicity with respect to the stress changes, however, is constrained by the occurrence of the 15 October 2013 Mw 7.2 Bohol Earthquake. Stress transfer models of the 2013 Bohol earthquake show a decrease of stress on the Negros source fault, and the effects of this are still unclear (Dianala, 2016). With this in consideration, only 20 months (*i.e.* from February 2012 to October 2013) of post-6 February 2012 Negros Earthquake seismicity were included in the earthquake data set.

Results of preliminary co-seismic *Coulomb* stress change analysis indicate that along-strike off-fault areas are where most after-

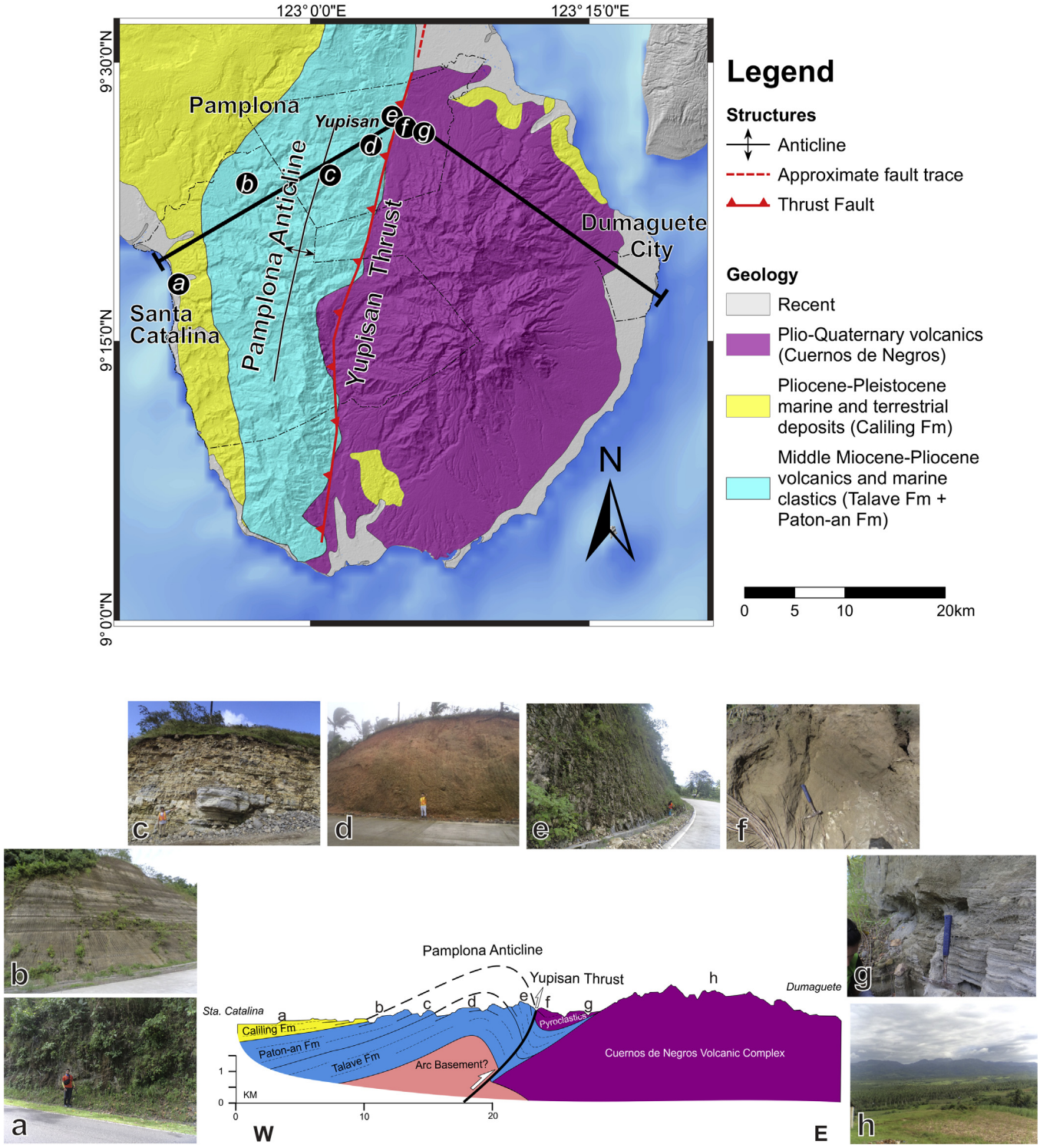

Fig. 10. Pamplona Anticline – Yupisan Thrust fold-thrust system established from a structural transect from the town of Sta, Catalina on the west to Dumaguete City to the east, passing through the town of Pamplona, manifested in the form of: (a) gentle westerly to northwesterly dips of coralline limestone beds of the Late Pliocene to Pleistocene Caliling Formation; (b) gentle westerly dips of sandstone – siltstone interbeds of the Early Pliocene Paton-an Formation that overlie the Caliling Formation to the east; (c) gentle easterly and southeasterly dipping calcareous sandstone - siltstone – mudstone interbeds of the Middle to Late Miocene Talave Formation; (d) strongly deformed beds of the Talave Formation, including numerous outcrop scale thrust faults and related folds; (e) steep easterly dips to vertical orientation of beds of calcareous clastic sequences of the Early Pliocene Paton-an Formation; (f) steep to moderate easterly dips and (g) flat-lying sequences of pyroclastic sandy layers associated to the Pleistocene to Quaternary Cuernos de Negros Volcanic Complex; (g) elevated, stratovolcanic dome of the Quaternary Cuernos de Negros Volcanic Complex viewed to the east. This configuration reveals an asymmetric fold (Pamplona Anticline) whose fold plane is inclined to the west and soled by a reverse fault here proposed to be named the Yupisan Thrust, the likely southern continuation of the Negros Oriental Thrust. Location of outcrops discussed and cross section line indicated in the Location Map zoomed out from Fig. 2 (coverage shown). SRTM data from Jarvis et al. (2008).

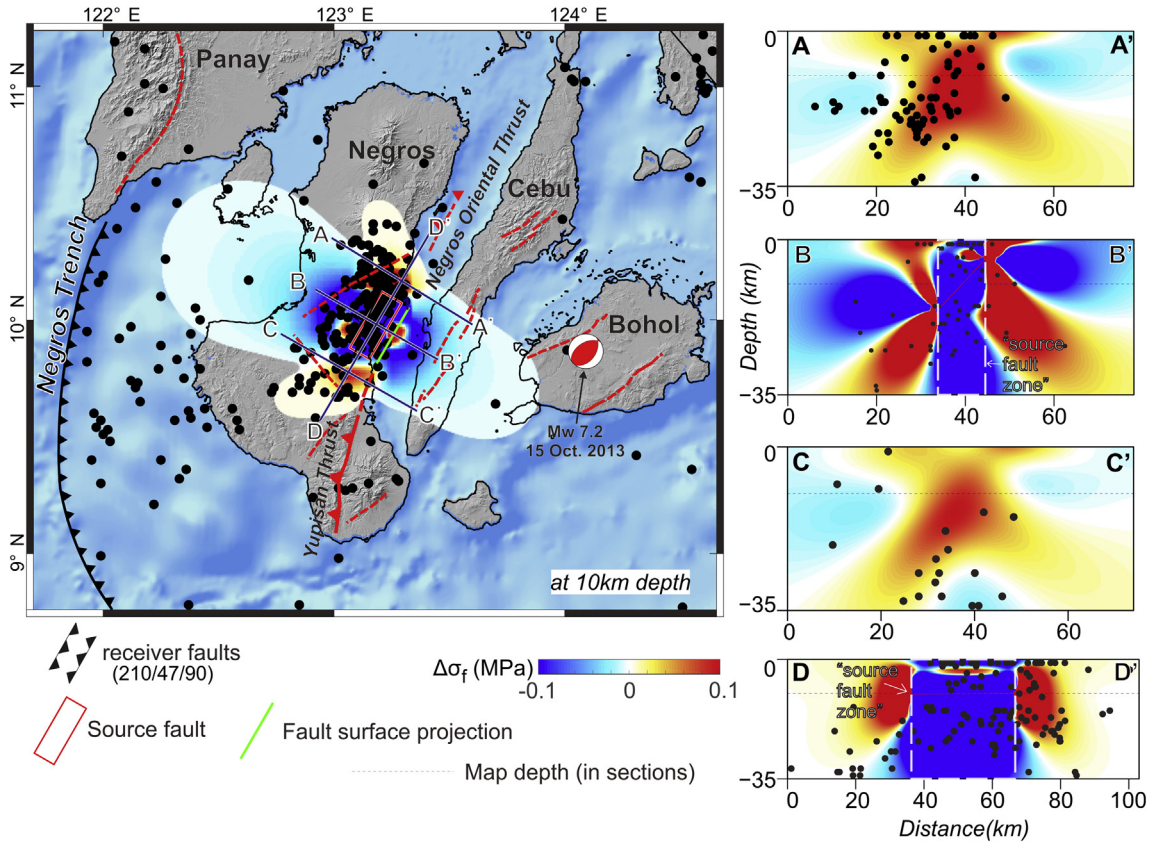

Fig. 11. Co-seismic static stress transfer model of the Mw 6.7 2012 Negros Earthquake on specified receiver faults (210° strike, 47° dip, 90° rake). Map shows stress change at 10 km depth, with corresponding cross-sections A-A' (north of fault), B-B' (mid-fault), C-C' (south of fault), and D-D' (along strike from south to north of fault). Cross section bandwidth is 20 km. The "source fault zone" is indicated by broken, white lines. Location and focal mechanism solution of Mw 7.2 2013 Bohol Earthquake also shown.

shocks are predictable by zones of co-seismic stress increase. This is most apparent in cross-sections **A-A′** and **C-C′** of Fig. 11, where there are stress increases of around 0.05 MPa and greater. However, within the zone directly above and below the source fault, as delineated in cross-sections **B-B′** and **D-D′** of Fig. 11, it is difficult to correlate aftershock distribution with stress changes, since we also find aftershocks in areas where stress has decreased (around $\geqslant$0.05 MPa). This is likely due to the real complexities (geometry, roughness, bedrock rheology, *etc.*) of the rupturing fault not captured by the source fault model, as well as to differences in the rupture mechanisms of the aftershocks that may not be similar to the assumed receiver faults (Catalli and Chan, 2012; Chan et al., 2012, 2017). Stress change in thrust faults also happen to be depth-dependent (Lin and Stein, 2004). Nevertheless, the model shows an increase of stress in southern Negros Island, along the Yupisan Thrust (Fig. 11). However, to date historical earthquake data do not indicate significant seismicity along this fault. This could be due to the variation of the crustal properties introduced by the volcanic system of Cuernos de Negros, or perhaps the seismic activity predicted by the model is yet to happen.

9. Discussion

The magnitude Mw 6.7 Negros Earthquake of 2012 bears important implications in addressing questions on fundamental seismotectonics, as well as on earthquake hazard assessment. This earthquake provides significant insights in better understanding the tectonic deformation of an arc-basin terrane, but at the same time serves as an eye opener in the evaluation of regions previously unrecognized as hosts to major and devastating earthquakes.

9.1. Seismotectonic implications

The earthquake revealed a structure previously unrecognized in earlier works. It showed that there exists a major reverse fault bounding the western sector of the Visayan Sea Basin. The recognition of the west-dipping Negros Oriental Thrust provides a strong argument to suggest that the western margin of the Visayan Sea Basin is presently being subjected to a compressional tectonic regime. This observation is in contrast with the erstwhile model that the Tañon Strait at the western section of the Visayan Sea Basin is a graben, bounded on both flanks by normal faults (*e.g.* Glocke, 1980; adopted by Rangin et al., 1989, see also Fig. 8) implying an extensional tectonic regime instead.

The geometries of the Negros Oriental Thrust and Yupisan Thrust (*i.e.* northeast-striking, northwest-dipping) and the shallow focal depth (10–15 km) of the East Negros Earthquake may suggest a back thrust structure affecting a back-arc basin in the context of the east-dipping Negros subduction system located to the west of the island. However, in less than 2 years, the neighbouring island of Bohol was hit by a magnitude Mw 7.2 earthquake on 15 October 2013 (Aurelio et al., 2013b; Rimando, 2015; Rimando et al., 2014). Like in the Negros Earthquake, the Bohol Earthquake revealed an active fault structure that has not been recognized in earlier works. The Bohol earthquake revealed the existence of the North Bohol Fault (PHIVOLCS, 2014), an east-dipping reverse fault deforming the southeastern border of the Visayan Sea Basin. Although the northeast-striking, east-dipping geometry and thrust mechanism of the newly revealed North Bohol Fault may not appear consistent with a back thrust system, it is certainly a strong argument that the Visayan Basin is now inversing under a compressional tectonic regime.

While F1 as seen on the seismic profiles appears to be a candidate that satisfies the FMS-determined fault parameters (Fig. 8A) of the generator of the Negros Earthquake, it is not impossible that the earthquake could have been produced by a paralleling fault in the system. However, the best the data available at this point could suggest is for the Negros Oriental – Yupisan Thrust System to be the best candidate capable of generating an earthquake of such magnitude, considering its extent horizontally, based on the field structural observations (transects – Figs. 9 and 10) and vertically, based on seismic profiles (Fig. 8) and hypocentral plots (Fig. 3).

9.2. Insights to earthquake hazard assessment of low seismicity regions

The occurrence of the Negros Earthquake in an area where no active faults have been previously recognized underscores the challenge of evaluating the earthquake risks of regions that are characterized by seemingly low potential for large magnitude earthquakes. Block motion vectors calculated from GPS campaigns in the central and southern Philippines (Duquesnoy et al., 1994; Kreemer et al., 2000; Rangin et al., 1999; Aurelio, 2001; Aurelio and Vigny, 2001) indicate an east-west to east-southeast-west-northwest directed principal stress axis, consistent with the northeast (North Bohol Fault) to north-northeast (Negros Oriental Fault – Yupisan Thrust) strikes of the faults and their reverse mechanism. However, calculated strain rates and fault slip rates in the region where the islands of Negros and Bohol are located are relatively low. But despite the low strain and fault slip rates, these neighbouring islands, less than 100 km apart, were struck by 2 successive large magnitudes earthquakes within a span of less than 2 years, which suggests that the earthquake probabilities in this region are being underestimated. Some authors emphasize the need to employ alternative approaches in earthquake risk assessment of regions situated in similar tectonic settings (*e.g.* Sugiyama et al., 2003; Shaw and Shearer, 1999) especially for regions underlying highly urbanized areas. Efforts of earthquake hazard assessment in Japan (*e.g.* Asada, 1991; Toda, 2013) indicate that earlier active fault maps tended to underestimate the potential of many regions in the Japanese archipelago because many of the earthquake generators have not been mapped and remain hidden (blind), and that these regions are characterized by very slow fault slip rates. Still others (*e.g.* Stein and Stirling, 2015; Michael, 2014; Frankel, 2013) highlight the need for better earthquake data collection and more long-term experimentation in undertaking time-dependent probabilistic earthquake hazard assessments.

10. Conclusions

The magnitude Mw 6.7 Negros Earthquake of 6 February 2012 has revealed an active fault structure underneath the island never before mapped on the surface. On the basis of seismic profiles in the Tañon Strait, correlated with the distribution of aftershock hypocenters, this structure, here proposed to be called the Negros Oriental Thrust, is a northeast striking, northwest dipping reverse fault operating under a compressive stress regime characterized by a northwest-southeast oriented principal stress axis direction. To the south, the Yupisan Thrust, recognized on the basis of the style of deformation affecting late Cenozoic limestones and calcareous clastic deposits underlying the southern Negros peninsula, is the likely southern extension of the Negros Oriental Thrust. Together, these large reverse faults serve as the sole thrust of an anticlinal fold whose axis is aligned parallel to the fault strike (Fig. 2). In central Negros, the Negros Oriental Thrust paired with the Razorback Anticline, promotes basin inversion on the western section of the Visayan Sea Basin. In southern Negros, the east-verging Yupisan Thrust – Pamplona Anticline thrust-fold system abuts into the Cuernos de Negros Volcanic Complex. The discovery of these previously unrecognized structures is key in understanding the seismotectonic setting of the region they affect. Furthermore, it highlights the necessity of paying more attention and exerting more efforts in earthquake hazards assessment of seemingly seismically quiet intraplate crusts, especially in regions where urbanized cities are situated.

Acknowledgments

We acknowledge the valuable support extended by Philex Mining Corporation (Philex), especially its Exploration Department headed by Redempta Baluda and its team based in Sipalay, southern Negros that provided logistical and technical provisions to the survey team, as well as humanitarian aid to victims within the first few days after the earthquake. We also thank the assistance provided by the Region 7 Office of the Mines and Geosciences Bureau (MGB-R7) and the many local government officials of Negros Oriental for field support and governmental coordination on site. The seismic profiles used in this work are courtesy of the Philippine Department of Energy (DOE), while fieldwork in southern Negros was facilitated and supported by the Energy Development Corporation (EDC). We sincerely thank the unwavering support extended by these two organizations. M. Aurelio is grateful for the assistance provided by the Philippine Air Force and its UH-1H "Huey" fleet from the Mactan Air Base in Cebu, in flying the team to some of the survey areas during the critical first 72 hours following the earthquake. We sincerely thank 2 anonymous reviewers whose constructive comments and suggestions have greatly improved the manuscript. M. Aurelio appreciates the assistance extended by Jasper Sunico during the revision of the manuscript. The Generic Mapping Tool GMT (Wessel and Smith, 1991, 1995) was used to produce certain figures. Shuttle Radar Topography Mission (SRTM) data in some maps come from Jarvis et al. (2008).

References

Abigania, M.I., Arpa, M.C., Basan, S., Bornas, M.A., Cahulogan, M., Catane, S., Daag, A., Del Monte, L.R., Garcia, F., Goetz, C., Hernandez, V., Lamella, R., Penarubia, H., Rivera, R., Pagtalunan, M., 2012. Damages, deformation and impacts of the 06 February 2012 M6.9 Negros Oriental Earthquake, Philippines. In: Proceedings of the 25th Annual Geological Convention – GEOCON 2012, Makati City, Philippines, 2–3 December 2012. Available in CD.

Argus, D.F., Gordon, R.G., DeMets, C., 2011. Geologically current motion of 56 plates relative to the no-net-rotation reference frame. Geochem. Geophys. Geosyst. 12, Q11001. http://dx.doi.org/10.1029/2011GC003751.

Asada, T., 1991. Some questions on active faults. Active Faults Res. 9, 1–3.

Aurelio, M.A., 1992. Tectonics of the Central Segment of the Philippine Fault: Structures, Kinematics And Geodynamics. Doctoral Dissertation, Université Pierre et Marie Curie, University of Paris VI., vol. 1–2, Copyright: T92–22 Memoires des Sciences de la Terre, Academie de Paris, France, 500 p.

Aurelio, M.A., 2000a. Tectonics of the Philippines revisited. J. Geol. Soc. Philippines 55 (3-4), 119–183.

Aurelio, M.A., 2000b. Shear partitioning in an island arc setting: constraints from Philippine Fault and recent GPS Data. Island-Arc 9, 585–598.

Aurelio, M.A., 2001. GPS velocities in Mindanao Island. J. Geol. Soc. Philippines 56 (3-4), 214–224.

Aurelio, M.A., Vigny, C., 2001. Global Positioning System station velocity variations in the Philippines attributed to seismic charging and intra-measurement deformation near active tectonic structures. Sylvatrop 11 (1&2), 51–70.

Aurelio, M.A., Barrier, E., Rangin, C., Müller, C., 1991. The Philippine Fault in the Late Cenozoic evolution of the Bondoc-Masbate-N. Leyte area, Central Philippines. J. SE Asian Earth Sci. 6/3-4, 221–238.

Aurelio, M.A., Peña, R.E., (Eds.), 2010. Geology of the Philippines, 2nd Ed. – vol. 1: Tectonics and Stratigraphy. Published by the Mines and Geosciences Bureau, Department of Environment and Natural Resources. Quezon City, Philippines.

Aurelio, M., Taguibao, K.J., Dianala, J.D., Sarande, R., Lucero Jr., A., 2012. The Magnitude 6.9 Negros Oriental Earthquake of 6 February 2012: Insights from Earthquake, Offshore Seismic and Onshore Structural Data. In: Proceedings of the 25th Annual Geological Convention – GEOCON 2012, Makati City, Philippines, 2–3 December 2012. Available in CD.

Aurelio, M.A., Peña, R.E., Taguibao, K.J.L., 2013a. Sculpting the Philippine archipelago since the Cretaceous through rifting, oceanic spreading, subduction, obduction,

collision and strike-slip faulting: contribution to IGMA5000. J. Asian Earth Sci. 7, 102–107. http://dx.doi.org/10.1016/j.jseaes.2012.10.007.
Aurelio, M.A., Rimando, J.M., Taguibao, K.J.L., Dianala, J.D.B., Berador, A.E., 2013b. Seismotectonics of the magnitude 7.2 Bohol Earthquake of 15 October 2013 from onshore, earthquake and offshore data: a key to discovering other buried active thrust faults. In: Proceedings of the 26th Annual Geological Convention – GEOCON 2013, Makati City, Philippines, 3–4 December 2013. Available in CD.
Bacolcol, T., Pelicano, A., Artemio Jr., L., Jorgio, R.The PHIVOLCS GPS Team, 2012. Interseismic and post-seismic deformation sssociated with 6 Feb 2012 M6.9 Negros Earthquake. In: Proceedings of the 25th Annual Geological Convention – GEOCON 2012, Makati City, Philippines, 2–3 December 2012. Available in CD.
Bourbie, T., Coussy, O., Zinszner, E., 1987. Acoustics of porous media. Institut Français du Pétrole publications, ISSN 0241–6069, Editions TECHNIP, ISBN 2710805162, 9782710805168, 334 p.
Bureau of Energy Development, 1986. Sedimentary Basins of the Philippines, their Geology and Hydrocarbon Potential, v. 3 - Basins of Visayas and Mindanao. Published by BED under the auspices of the World Bank, 305 p.
Cardwell, R.K., Isacks, B.L., Karig, D.E., 1980. The spatial distribution of earthquakes, focal mechanism solutions and subducted lithosphere in the Philippine and northeastern Indonesian Islands. In: The Tectonic and Geologic Evolution of Southeast Asian Seas and Islands, Part 1. In: Hayes, D.E. (Ed.), . Am. Geophys. Union Monograph, vol. 23, pp. 1–35.
Castillo, P.R., Escalada, P.P., 1979. Geology of Southwestern Negros Island. Philippine Bureau of Mines Technical Information Series No. 4/79, 22p.
Catalli, F., Chan, C.-H., 2012. New insights into the application of the Coulomb model in real-time. Geophys. J. Int. 188 (2), 583–599. http://dx.doi.org/10.1111/j.1365-246X.2011.05276.x.
Chan, C.-H., Wang, Y., Almeida, R., Yadav, R.B.S., 2017. Enhanced stress and changes to regional seismicity due to the 2015 Mw 7.8 Gorkha, Nepal, earthquake on the neighbouring segments of the Main Himalayan Thrust. J. Asian Earth Sci. 133, 43–55. http://dx.doi.org/10.1016/j.jseaes.2016.03.004.
Chan, C.-H., Wu, Y.-M., Wang, J.-P., 2012. Earthquake forecasting through a smoothing Kernel and the rate-and-state friction law: application to the Taiwan region. Natural Hazards Earth Syst. Sci. 12, 1–13. http://dx.doi.org/10.5194/nhess-12-1-2012.
Corby, G.W., Kleinpell, R.M., Popenoe, W.P., Merchant, R., William, H., Teves, J., Grey, R., Daleon, B., Mamaclay, F., Villongco, A., Herrera, M., Guillen, J., Hollister, J.S., Johnson, H.N., Billings, M.H., Fryxell, E.M., Taylor, E.F., Nelson, C.N., Birch, D.C., Reed, R.W., Marquez, R., 1951. Geology and oil possibilities of the Philippines Technical Bulletin 21. Philippine Bureau of Mines, Department of Agriculture and Natural Resources, p. 365.
Daag, A., Bacolcol, T., Nakata, T., Cahulogan, M., Rivera, D., Villahermosa, R.L., Deposoy, C., Ramos, J.E., 2012. Sub-aerial and sub-marine landslides triggered by the February 6, 2012 Negros Oriental Earthquake: assessment and implications. In: Proceedings of the 25th Annual Geological Convention – GEOCON 2012, Makati City, Philippines, 2–3 December 2012. Available in CD.
Das, S., Henry, C., 2003. Spatial relation between main earthquake slip and its aftershock distribution. Rev. Geophys. 41, 3–23.
Dianala, J.D.B., 2016. Associating seismicity with static stress transfer from the February 2012 Negros and October 2013 Bohol earthquakes Masters Thesis. National Institute of Geological Sciences, University of the Philippines, Diliman, Quezon City. July 2015.
Duquesnoy, T., Barrier, E., Kasser, M., Aurelio, M.A., Gaulon, R., Punongbayan, R.S., Rangin, C.the French-Philippines Cooperation Team, 1994. Detection of creep along the Philippine Fault: first results of geodetic measurements in Leyte Island. Geophys. Res. Lett. 21 (11), 975–978.
Dziewonski, A.M., Chou, T.-A., Woodhouse, J.H., 1981. Determination of earthquake source parameters from waveform data for studies of global and regional seismicity. J. Geophys. Res. Solid Earth 86, 2825–2852.
Ekström, G., Nettles, M., Dziewoński, a.M., 2012. The global CMT project 2004–2010: centroid-moment tensors for 13,017 earthquakes. Phys. Earth Planet. Inter. 200–201, 1–9.
Frankel, A., 2013. Comment on "Why earthquake hazard maps often fail and what to do about it" by S. Stein, R. Geller, and M. Liu. Tectonophysics 592, 200–206. http://dx.doi.org/10.1016/j.tecto.2012.11.032.
Freed, A.M., 2005. Earthquake triggering by static, dynamic, and postseismic stress transfer. Annu. Rev. Earth Planet. Sci. 33, 335–367.
Gemal, G.F., Queaño, K.L., Mercado, G.M.P., Telles, C.J.R., Guarino, C.J.G., Gatdula, R.C., Padrones, J.T., Sanchez, M.P., Guotana, J.M.R., Dimalanta, C.B., Ramos, N.T., Faustino-Eslava, D.V., Yumul Jr., G.P., 2012. The February 6, 2012 Earthquake-induced landslides in Northern Negros Oriental, Philippines: Insights from geologic and geomorphic controls. In: Proceedings of the 25th Annual Geological Convention – GEOCON 2012, Makati City, Philippines, 2–3 December 2012. Available in CD.
Gervasio, F.C., 1967. Age and nature of orogenesis in the Philippines. Tectonophysics 4 (1), 379–402.
Global Centroid Moment Tensor (CMT) Project. Accessible at: <http://www.globalcmt.org/CMTsearch.html>.
Glocke, A., 1980. Geology and hydrocarbon prospects of the Visayan Basin. Appendix V: Results of seismic interpretation Unpublished Report. Manila Bureau of Energy Development, p. 77.
Hall, R., 2002. Cenozoic geological and plate tectonic evolution of SE Asia and the SW Pacific: computer-based reconstructions, model and animations. J. Asian Earth Sci. 20 (4), 353–431.
Harris, R.A., 1998. Introduction to special section: stress triggers, stress shadows, and implications for seismic hazard. J. Geophys. Res. 103, 24347–24358.
Holloway, N.H., 1982. The North Palawan Block, Philippines: its relation to the Asian mainland and its role in the evolution of the South China Sea. Geol. Soc. Malaysia Bull. 14, 19–58.
Jarvis, A., Reuter, H.I., Nelson, A., Guevara, E., 2008. Hole-Filled Seamless SRTM Data V4. International Centre for Tropical Agriculture (CIAT). Available at: <http://srtm.csi.cgiar.org>.
Kreemer, C., Holt, W.E., Goes, S., Govers, R., 2000. Active deformation in eastern Indonesia and the Philippines from GPS and seismicity data. J. Geophys. Res. 105 (B1), 663–680.
Kreemer, C., Kreemer, W.E., Haines, A.J., 2003. An integrated golabl model of present-day plate motions and plate boundary deformation. Geophys. J. Int. 154, 8–34.
Lin, J., Stein, R.S., 2004. Stress triggering in thrust and subduction earthquakes and stress interaction between the southern San Andreas and nearby thrust and strike-slip faults. J. Geophys. Res. 109, 1–19.
Marsden, D., 1989. Layer cake depth conversion. Lead. Edge 8 (1), 10–14. http://dx.doi.org/10.1190/1.1439561.
Melendres, M, Jr. and Barnes, H., 1957. Geology and Coal Resources of the Calatrava-Toboso Region, Occidental Negros. Philippine Bureau of Mines Special Publication Series, 12 – Coal, 50p.
Michael, A.J., 2014. How complete is the ISC-GEM Global Earthquake Catalog? Bull. Seismol. Soc. Am. 104, 1829–1837. http://dx.doi.org/10.1785/0120130227.
Okada, Y., 1992. Internal deformation due to shear and tensile faults in a half-space. Bull. Seismol. Soc. Am. 82, 1018–1040.
Philippine Institute of Volcanology and Seismology, 2012. Active Faults Map of the Philippines Accessible at: <http://www.phivolcs.dost.gov.ph>.
Pinet, N., 1990. Un exemple de grand decrochement actif en contexte de subduction oblique: la faille Philippine dans se partie Septentrionale Ph.D. Dissertation. Université. de Nice – Sophia Antipolis, France, p. 390.
Pinet, N., Stephan, J.F., 1990. The Philippine wrench fault system in the Ilocos Foothills, northwestern Luzon, Philippines. Tectonophysics 183, 207–224.
Porth, H., Müller, C., von Daniels, C., 1989. The sedimentary formations of the Visayan Basin, Philippines. Geologisches Jahrbuch Reihe B, Heft 70, 29–88.
Quebral, R.D., 1994. Tectonique du segment meridional de la faille philippine, Mindanao Oriental, Philippines: passage d'une zone de collision à une zone de décrochement Thèse de doctorat. Université Pierre et Marie Curie, Paris, France.
Rangin, C., Porth, H., Müller, C., 1989. Neogene geodynamic evolution of the Visayan Region. Geologisches Jahrbuch Reihe B, Heft 70, 7–27.
Rangin, C., Le Pichon, X., Mazzotti, S., Pubellier, M., Chamot-Rooke, N., Aurelio, M., Walpersdorf, A., Quebral, C., 1999. Plate convergences measured by GPS across the Sundaland/Philippine Sea Plate deformed boundary: the Philippines and eastern Indonesia. Geophys. J. Int. 139, 296–316.
Rimando, J.M., 2015. Ground deformation associated with the October 15, 2013, Magnitude 7.2 Bohol Earthquake, Bohol Island, Philippines Masters Thesis. National Institute of Geological Sciences, University of the Philippines, Diliman, Quezon City. March 2015.
Rimando, J., Aurelio, M.J.A., Taguibao, K.J., Dianala, J.D., 2014. Geological manifestations of a hidden thrust fault associated to the October 15, 2013 Mw 7.2 Bohol Earthquake, Central Philippines. In: Proceedings of the 11th Annual Meeting of the Asia-Oceania Geosciences Society, 28 July – 1 August 2014, Sapporo, Japan.
Rimando, R., Lim, R.B., Garduque, R.J., Rimando, J.M., 2013. Ground rupture of the February 06, 2012 Negros Earthquake. In: Proceedings of the 26th Annual Geological Convention – GEOCON 2013, Makati City, Philippines, 3–4 December 2013. Available in CD.
Ringenbach, J.C., 1992. La Faille Philippine et les châines en décrochement associés (centre et nord de Luzon): Evolution cénozoique et cinématique des déformations quaternaires Ph.D. Dissertation. Université. de Nice – Sophia Antipolis, France, p. 316.
Ringenbach, J.C., Stephan, J.F., Maleterre, P., Bellon, H., 1990. Structure and geological history of the Lepanto-Cervantes releasing bend in the Abra River Fault, Luzon Central Cordillera, Philippines. Tectonophysics 183, 225–241.
Seno, T., 1977. The instantaneous rotation vector of the Philippine Sea Plate in relation to the Eurasian Plate. Tectonophysics 42, 209–226.
Shaw, J.H., Shearer, P.M., 1999. An elusive blind-thrust fault beneath Metropolitan Los Angeles (California). Science 283, 1516–1518.
Steacy, S., Gomberg, J., Cocco, M., 2005. Introduction to special section: stress transfer, earthquake triggering, and time-dependent seismic hazard. J. Geophys. Res. 110, B05S01.
Stein, R., 1999. The role of stress transfer in earthquake occurrence. Nature 402, 605–609.
Stein, R.S., Stirling, M.W., 2015. Seismic hazard assessment: honing the debate, testing the models. Eos 96. http://dx.doi.org/10.1029/2015EO031841.
Stein, R.S., Barka, A.A., Dieterich, J.H., 1997. Progressive failure on the North Anatolian fault since 1939 by earthquake stress triggering. Geophys. J. Int. 128, 594–604.
Stein, R.S., King, G.C., Lin, J., 1992. Change in failure stress on the southern San Andreas fault system caused by the 1992 magnitude 7.4 Landers earthquake. Science 258, 1328–1332.
Sugiyama, Y., Mizuno, K., Nanayama, F., Sugai, T., Yokota, H., Hosoya, T., Miura, K., Takemura, K., Kitada, N., 2003. Study of blind thrust faults underlying Tokyo and Osaka urban areas using a combination of high-resolution seismic reflection profiling and continuous coring. Ann. Geophys. 46 (5), 1071–1085.
Toda, S., 2013. Current issues and a prospective view to the next step for long-term crustal earthquake forecast in Japan. J. Geol. Soc. Jpn. 119, 105–123 (in Japanese with Englis abstract).

Toda, S., Enescu, B., 2011. Rate/state Coulomb stress transfer model for the CSEP Japan seismicity forecast. Earth, Planets and Space 63, 171–185.
Toda, S., Lin, J., Stein, R.S., 2011. Using the 2011 Mw 9.0 off the Pacific coast of Tohoku Earthquake to test the Coulomb stress triggering hypothesis and to calculate faults brought closer to failure. Earth, Planets Space 63, 725–730.
Toda, S., Stein, R.S., 2013. The 2011 M = 9.0 Tohoku oki earthquake more than doubled the probability of large shocks beneath Tokyo. Geophys. Res. Lett. 40, 2562–2566.
Toda, S., Stein, R.S., Beroza, G.C., Marsan, D., 2012. Aftershocks halted by static stress shadows. Nat. Geosci. 5. http://dx.doi.org/10.1038/NGEO1465.
Toda, S., Stein, R.S., Richards-Dinger, K., Bozkurt, S.B., 2005. Forecasting the evolution of seismicity in southern California: animations built on earthquake stress transfer. J. Geophys. Res. 110, 1–17.
Wells, D., Coppersmith, K., 1994. New empirical relationships among magnitude, rupture length, rupture width, rupture area, and surface displacement. Bull. Seismol. Soc. Am. 84, 974–1002.
Wessel, P., Smith, W.H.F., 1991. Free software helps map and display data. EOS Trans. Am. Geophys. Union 72 (441), 445–446.
Wessel, P., Smith, W.H.F., 1995. New version of the Generic Mapping Tools released. EOS Trans. Am. Geophys. Union 76, 329.
Yu, S.-B., Hsu, Y.-J., Bacolcol, T., Yang, C.-C., Tasai, Y.-C., Solidum, R., 2013. Present-day crustal deformation along the Philippine Fault in Luzon, Philippines. J. Asian Earth Sci. 65, 64–74.